Luminescence dating of irrigation systems: application to a qanat in Aragón, Spain

I. K. Bailiff [1] *, C. M. Gerrard [1], A. Gutiérrez[1], L. M. Snape-Kennedy[1] and K. N. Wilkinson[2]
[1]Department of Archaeology – Durham University, Durham DH1 3LE, UK.
[2]Department of Archaeology – University of Winchester, Winchester, Hampshire S022 4NR, UK.
* Corresponding author: Ian.Bailiff@durham.ac.uk

Abstract

Optically stimulated luminescence (OSL) techniques have been applied to investigate the potential for dating the deposition of upcast mounds associated with qanat ventilation shafts at the site of a medieval qanat located in Aragón, Spain. Coarse quartz grains, extracted from sediment samples taken from excavated sections of several mounds, possessed sufficiently strong OSL to enable an evaluation of equivalent dose by applying the single aliquot regenerative procedure to small aliquots, each containing an individual bright grain. The OSL dates for both palaeosol and overlying upcast indicate that a chronostratigraphic record has been preserved within the mounds investigated, and micromorphological analysis of thin sections of sediment blocks taken from the mounds is shown to provide an essential means of verifying the characteristics of the strata, in particular, the critical interface of upcast and the ancient ground surface. The earliest OSL dates for basal deposits taken from two separate sections of the same mound are in agreement, placing the mound construction during the first half of the 13th century A.D. However, in two other mounds the OSL dates for the deposition of upcast are internally consistent with the stratigraphy but significantly later, dating to the 16th and 17th centuries A.D. We interpret the differences between the dates for the upcast deposition to be the result of partial erosion of the upper shaft and later repair of the mounds, and this finding underlines the importance of both examining multiple mounds in the same qanat system and the internal structure of each sampled mound. This exploratory work demonstrates the potential for wider application of OSL for dating this important type of subterranean irrigation feature in the study of both the archaeology of human settlement and palaeoenvironmental change in arid regions.

1. Introduction

Water is one of the key resources that structures human activity and therefore ancient irrigation systems constitute a central element in the study of human settlement in the past. However, our understanding of the history of the development of water systems and the transfer of water technologies across regions are often significantly hampered by not knowing when they were built. The qanat (also foggara, karez, khittara and other variants) is one form of engineered hydraulic irrigation system that is characterised by a subterranean channel, and archaeological remains of such features are widespread from the Near East to the Mediterranean basin and further afield in Central Asia and the New World (English, 1968). This hydraulic technology is reported to have been introduced in the early 1st millennium BC in Persia and progressively adopted in arid regions both eastwards and westwards, and its appearance seemingly occurred later in Spain during the 1st millennium AD (Glick, 1970). With few exceptions in which dating is implied by indirect association with adjacent settlements or the incorporation of diagnostic artefacts in upcast sediment, individual qanats have proven almost impossible to date. This absence of a chronological framework hampers both our understanding of technology transfer, as well as the study of local settlement and landscape evolution and the temporal correlation of land use with climatic and palaeoenvironmental data. The method of construction of the qanat has remained essentially unchanged; vertical shafts are dug at intervals of 15-150 m to provide ventilation for the tunnel and as a means of transferring upcast from the tunnel to the ground surface, forming a 'doughnut' of sediment around the rim, with further upcast being added during cleaning and maintenance. Given these processes, the surface shaft mounds potentially contain a sequence of deposits collected periodically from the tunnel, starting with initial construction and persisting until the last maintenance episode, less any material lost by surface erosion. In the only known published application of luminescence to date the deposition of upcast associated with a qanat, Fattahi et al. (2011) obtained OSL dates for samples from a shaft and mound that were pre-Holocene and, although these dates were consistent with the stratigraphy within the shaft, they were much earlier than the estimated date of construction of the qanat. In this paper we discuss the application of OSL and micromorphological techniques in a pilot study which examines the internal structure of upcast mounds within a qanat located in the Huecha Valley, Aragón, Spain. We will address specifically whether a chronostratigraphy can be constructed for mounds from OSL dates and evaluate the potential for further applications of this OSL-based approach to dating the construction and use of qanats.

2. The Bureta qanat

The post-Roman qanat (ca 170 m long) examined in this study is located in the Huecha Valley (Fig. SM1) near the village of Bureta, in Zaragoza province, Aragón (Fig. 1) and located in the north-east of Spain (Gerrard, 2011). Within the valley a large-scale landscape archaeology project (Gerrard and Gutiérrez, 2012) has been investigating population, economic and environmental change during the later Holocene in one of the most arid regions of Europe. In the southwest of this region, the Moncayo mountain range peaks at 2,316 m and is formed of Palaeozoic metamorphic rock. On the foothills, sandstones and limestone rocks of Triassic and Jurassic age dominate and the dry flat Huecha Valley extends for some 35 km to the northeast towards the Ebro River. The geology of the area is ideal for sourcing and managing water supplies, with soft Tertiary marls and gypsums that facilitated the excavation of tunnels and shafts for accessing the aquifer. The Bureta qanat is a unique irrigation feature in the Huecha Valley (Gerrard, 2011), where a complex network of dams, channels, storage ponds, and watermills of different periods have been identified and documented, all of which have been adapted to the terrain and geomorphology, but also evolved as a response to climate change (e.g., Little Ice Age; Burillo et al., 1986; Gutiérrez and Peña 1998; Peña et al., 2000), and land-use and landscape management change, as gleaned from sedimentary records (Wilkinson et al., 2005). Although irrigation networks within the Huecha Valley are well documented for the medieval and post-medieval period (Gerrard, 2011), there is no documentary reference to the construction of the Bureta qanat

and, on the basis of the adoption of an Islamic hydraulic technology, it is assumed to be associated with the availability of such expertise after the 8th century AD.

3. Fieldwork

Of the six shafts in the Bureta qanat, three mounds (Fig. 3; S2-S4) were selected for investigation. The sampling of the shaft mounds was performed in two phases of fieldwork. In the first, mounds S2 (391-2) and S4 (391-1) were sectioned and sampled for OSL, and basic details of the lithology were collected, including visual identification of the contact between the upcast and the buried land surface. In the second phase of sampling mounds S2 (different position) and S3 were hand excavated, cleaned, drawn at 1:20 scale and photographed. Field descriptions of both sections were undertaken using standard protocols, noting the texture, sorting, inclusions, structure, boundary types (Jones et al., 1999) and Munsell colour (Munsell 1952) of each deposit.

Samples for both OSL and micromorphological analysis were extracted as blocks, cut into the prepared section to a depth of at least 10 cm. The blocks, once extracted, were wrapped immediately in opaque plastic sheet and subsequently trimmed, sealed and packed under subdued lighting conditions for transport. At the time of excavation the moisture content of all the blocks was very low.

The Stratigraphic Units (SU) identified in each of mounds S2 and S3 are illustrated in Fig. 2a,b (further details are given in the Supplementary Material, Fig. SM2 and Tables SM 1a and 1b). The upcast deposits varied in texture, colour and sorting, but are generally composed of calcareous silty clay to fine sand with the clay often present as granular aggregates. The mound deposits are poorly sorted and contain and are characterised by moderate void space, both features that reflect their anthropogenic depositional origin. Moderately organic humic layers and roots were present in the upper layers and it is clear that this vegetation helped to stabilise the mounds. The stratigraphic units comprising the mounds ranged between 10 and 50 cm in thickness and were separated by sharp boundaries, indicating that they formed as discrete depositional events. Within the section of S2 (Fig. 3a) the four stratigraphic units identified showed no evidence for erosion and weathering between different phases of upcast deposition, however, and the transition from the basal palaeosol to the first phase of upcast had a sharp, undulating boundary, indicating that truncation had occurred prior to burial by upcast. A more detailed discussion of the sediment microstructure is continued in the following section.

4. Micromorphological Investigation

Thin sections were prepared (Thin Section Micromorphology Laboratory, University of Stirling) using standard preparation procedures (http://www.thin.stir.ac.uk/category/methods/) of two block samples of unconsolidated sediment taken across the transition from exposed ground surface to burial by upcast deposition in S2 (391-3.2M) and S3 (391-4.3M); Fig. 2a,b. Visual analysis was initially performed under normal lighting to identify sub-units based on colour and texture and subsequently under plain-polarised light (PPL), cross-polarised light (XPL) and oblique incident light (OIL) between x4 and x500 magnification using a Leica petrological microscope. The strata in each were described semi-quantitatively using reference images and description criteria following Bullock et al. (1985), Courty et al. (1989) and Stoops et al. (2010). Five units were identified (a more detailed description of which is given in the Supplementary Material, Section 3).

In the exposed section of mound S2 (391-3.2M), the lowest unit (Fig. 2a, SU 4) is characterised by a mid-grey colour and coarse texture, while the upper limit shows evidence for bioturbation, suggesting that it was exposed for an extended period of time before burial, and it is likely that the upper part of the palaeosol (SU 4 in Fig. 2a and SU 4b identified in the thin section, Fig. SM3a). In mound S3, what was thought during excavation to be the contact between the original ground surface and upcast (Fig. 2b, SU 7 and SU 6) was in fact two phases of upcast accumulation. Evidence for the incorporation of Mg and Fe in the lower unit

suggests a period of exposure before burial (Courty et al., 1989: 185). The sharp horizontal boundary between upcast deposits (SU 7 and SU 6) in mound S3 provides separate accumulation events. However the lack of disturbance or bioturbation on the upper contact of SU4 suggests a relatively short period of exposure before deposition of upcast deposits.
In the thin sections for both S2 and S3 mounds, the clods identified in upcast deposits (S2; SU 3 and S3; SU 6) varied from fine-grained micritic calcareous rich silts/clays to poorly sorted fine sandy silt/clays (Supplementary Material, Figs SM3a-e). Many of the clods had clay laminations and these microstructures are usually indicative of slow-moving water conditions (Reineck and Singh, 1980; van der Meer and Menzies, 2011). Such laminations could have been formed inside the qanat tunnel, running parallel to its basal surface, and retained during the transfer of upcast to the mound, albeit in different orientation due to the displacement of the clods.
Each deposit type showed a mix of quartz concentration, texture, sorting and shape, with fine and coarse sand textures ranging from rounded (long transport history) to angular (short transport history). A number of fine-grained clods were present within the palaeosol (SU 4) and upcast deposits (SU 3 and SU 6) and the quartz grains within them are likely to have experienced little or no exposure to daylight associated with the deposition of upcast. Occasional fragments of quartz-rich rock were also present in the deposits and similarly the light exposure history of any disaggregated quartz grains released from them is uncertain. Examination of the thin sections also confirmed the presence of other mineral inclusions such as K-feldspars, micas, calcite, epidote and sporadic fragments of various organic materials (shell, roots and charcoal). The presence of poorly sorted material of different origins, together with microanalysis of the sediment structure, indicates that overall these mound strata have a structure similar to colluvium, with the attendant issues for OSL dating of non-uniform exposure to daylight.

5. OSL Investigation

5.1 Methodology

OSL dating measurements were performed on coarse grains of quartz extracted from the upcast deposits and underlying palaeosols. A summary of the experimental work is presented in this section and further technical details are provided in the Supplementary Material.

5.2 Sample preparation

The block samples were trimmed of surface material (>10mm) and the sediment extracted under subdued red lighting conditions, where the sub-surface material was used for dose rate assessment. The larger blocks obtained in the second phase of fieldwork (391-3 and -4) were sub-sampled from a cut slot of ca 12 mm depth and for the blocks taken from the first phase (391-1 and -2), the thickness of the sub samples ranged from 10 to 60 mm in thickness. Tube samples which were taken from the upper strata of the mound (Fig. 2) were not analysed.
Coarse quartz grains were extracted from the sediment by applying the standard inclusion technique (Aitken, 1998). Most of the samples were sufficiently coarse to yield adequate quantities of grains within the 150-200 μm and 200-355 μm size ranges, the larger grains being preferred because they increased the likelihood of obtaining well resolved OSL decay curves from individual grains . Small aliquots of etched grains were deposited onto stainless steel discs that had been lightly sprayed with silicone oil, dispersing the grains to avoid clustering.

5.3 Equivalent dose

The equivalent dose, D_e, was determined by applying a single aliquot regenerative procedure (SAR), similar to that described by Murray and Wintle (2000, 2003), but with some minor differences (Supplementary Material, Table SM3a). The SAR procedure was extended by the use of an OSL scanner to determine the number of bright grains contributing to the detected luminescence in each aliquot (Bailiff et al, 2014; Supplementary Material, Section 3.2). A

dose recovery experiment (Wintle and Murray, 2006) was performed using three different preheat temperatures selected between 180 and 240 °C to examine the dependence of the values of D_e on preheat temperature and to establish the extent of intrinsic overdispersion, σ_i, of the mean values obtained for the ratio D_e/D_a (where D_a is the applied dose).

5.4 Dose rate

The average total dose rate to coarse quartz grains, $\dot{D}_{tot}$, was assessed taking into account lithogenic radionuclide sources located a) within the grains, emitting alpha and beta radiation and b) within the sediment medium external to the grains, emitting beta and gamma radiation, and c) cosmic radiation. External grain beta dose rates were measured directly using beta thermoluminescence dosimetry (β-TLD; Supplementary Material, Section 3.4). In the β-TLD technique, the active sample volume relevant to the measurement of the external dose rate is ~0.25 cm^3, and for coarse-grained sediments, such as upcast, replicate measurements with separately sampled volumes provided a means of testing for significant heterogeneity in radionuclide distribution (Bailiff et al., 2014). The beta dose rate was also determined indirectly by measuring the specific activities of the lithogenic radionuclides (discussed below) and calculating the infinite medium dose rates using published conversion factors (Adamiec and Aitken, 1998) and additional calculations (Bailiff, 2007).

High resolution γ–ray spectrometry was used to measure the average specific activities (Bq kg^{-1}) of lithogenic radionuclides contained in the sediment samples, and their values were used to calculate the contemporary dose rate within layers of infinite (β, γ) and semi-infinite thickness (γ). A nominal value of the average burial moisture content (3±3%) was assumed for both palaeosol and upcast. For each dating sample volume, the gamma dose rate, $\dot{D}_{\gamma}$, was calculated using a multiple-layer gamma dose rate model that uses geometry coefficients calculated by Løvborg and given in Aitken (1985; Appendix H). The spreadsheet-based model (Bailiff et al., 2014) was applied to calculate the gamma dose rate at each sample position in the (contemporary) 'static' configuration, taking into account sediment strata of differing radionuclide content within ~50 cm of the sample position. Since the static configuration does not necessarily represent the time-averaged dose rate following initial burial (apart from the adjustments made to account for moisture content), the time-averaged combined gamma and cosmic dose rate was estimated using a simple dynamic model (Supplementary Material, Section 3.4.3; Bailiff et al., 2014) where the effect of the development of the overburden from burial of the buried land surface to the present mound surface on the gamma and cosmic dose rates is taken into account.

5.5 OSL age calculation

The luminescence ages were calculated by evaluating the quotient of the equivalent dose D_e and the average total dose rate, $\dot{D}_{tot}$. The associated type A ($\pm\sigma_A$) and B ($\pm\sigma_B$) standard uncertainties (ISO 1993) were calculated using a procedure based on an analysis of the propagation of experimental errors, similar to that described by Aitken (1985), and also taking into account the sample conditions during their burial history that potentially may affect the values of parameters used in age calculation.

5.6. Results

5.6.1 OSL characteristics

The OSL decay curves for coarse grains extracted from both upcast and palaeosols consistently contained a dominant fast component (Supplementary Material, Fig. SM4a). The OSL signal intensities were generally not sufficiently strong to test for the influence of the medium or slow decay components by applying the early background (EBG) subtraction procedure (Ballarini et al., 2007). The acceptance criteria (Wintle and Murray, 2006; Jacobs et al., 2006) for the recycling ratio, set at ±10% of unity, was met by a high proportion of the samples and the ratio averaged over all samples was 0.98±0.012 (listed for each sample in

Table SM3b, Supplementary Material). In the dose recovery experiments, a preheat plateau was obtained with the majority of the samples for preheat temperatures, investigated between 200 and 240 °C and in most cases the preheat temperature applied for D_e evaluation was 220 °C. The overdispersion in the distribution of the values of the ratio D_e/D_a (where D_a is the applied dose) ranged between 0% and 23% (σ_i, Table 1).

5.6.2 Equivalent dose

The central dose model (CDM), the minimum dose model (MDM) and in one case the finite mixture model (FMM) were applied to calculate the weighted mean value of D_e. (Galbraith et al., 1999), taking into account the results of the descriptive statistical analysis discussed below, the criteria proposed by Bailey and Arnold (2006) and the more recent experience with irrigation deposits (Huckleberry and Rittenauer, 2014; Huckleberry et al., 2012; Berger et al., 2009; Rittenauer, 2008). The key parameters associated with the D_e values are listed in Table 1, and further statistical data are included in the Supplementary Material (Table SM3b).

The CDM was initially applied to estimate the overdispersion, σ_b, in the distribution of D_e values obtained for each sample (col. 6). The estimated uncertainty associated with each D_e value was calculated by combining in quadrature the intrinsic uncertainty, σ_i , for that sample (the overdispersion in the distribution of D_e values determined in the dose recovery experiment) and the instrumental uncertainty (the standard error of the mean value of D_e determined following the SAR procedure). The uncertainties, σ_i and σ_b for each sample are listed in Table 1 as percentages (cols. 6 and 7), and the number of aliquots containing one dominant bright grain (1gr) yielding the D_e values used in these calculations is also given in the adjacent column (n, 1gr). The weighted mean value of D_e and the model applied to calculate it are given in cols 9 and 10 respectively, the selection of the model being based on an assessment of the mode of sediment deposition, the overdispersion and the weighted skewness in the distribution of D_e values, as discussed further below.

The degree of skewness (weighted, c; Arnold and Roberts, 2009; Bailey and Arnold, 2006) was calculated using D_e values obtained with aliquots containing a dominant individual bright grain (1gr) and also those containing up to several bright grains (Supplementary Material, Table SM3b). Only one aliquot exhibited a value of c that exceeded the critical value ($c_{crit}= 2\sigma_c$), although several others exceeded 50% of this value. For brevity we focus in this section on an analysis of the results obtained with aliquots containing one dominant bright grain used in calculation of the OSL ages, but the data provided by those aliquots with several bright grains (2-4) were also used to support the overall analysis (Supplementary Material, Table SM3b).

Where palaeosols were formed under the conditions of progressively aggrading deposits without subsequent significant disturbance, a proportion of the quartz grains extracted from them were expected to have been well-bleached before burial, as reflected in the overdispersion (OD) and skewness of the D_e distributions (Bailey and Arnold, 2006; Bateman et al., 2007). In contrast, the light exposure history of grains extracted from upcast deposits is likely to be more complex, and the degree of partial bleaching uncertain because of the particular mode of deposition associated with qanat construction and maintenance. On the basis of the micromorphological examination of mound sections for S2 (391-3) and S3 (391-4), discussed above, samples 3.1.1 (and by association, 2.1) and 3.1.2 from shaft mound S2 were assessed to have been taken from palaeosols and all the remaining samples from upcast deposits, including 4.1.1 and 4.1.2 that at the time of excavation had been thought to comprise palaeosols.

Of the strata expected to be more uniformly optically bleached at deposition, and hence with lower overdispersion (OD) in D_e values (σ_b; Table 1, col. 7), the samples extracted from the deeper levels of palaeosol (3.1.1 and 2.1) were expected to fall into this category. The overdispersion in D_e values for sample 3.1.1 is higher (29%) than that expected for well-

bleached sediments (ca 20%; Arnold and Roberts, 2009), but this is sustained by a single outlying D_e value and the OD reduces to 21% when removed (with a corresponding reduction in skewness, discussed further below). For aliquots containing more than one bright grain (Supplementary Material, Table SM3b; 2-4 gr, n=4) the OD is lower (21%), and although in part this can be attributed to the effects of grain averaging (Arnold et al., 2012), the secondary data, albeit limited, suggest that the majority of grains were likely to have been well bleached. Similarly, in the case of sample 2.1, the removal of a single outlying D_e value reduces the OD in the distribution of D_e values from 46% to 0%. However, in this case, the OD in the D_e distribution obtained with aliquots containing more than one bright grain (Supplementary Material, Table SM3b; 2-4 gr; n=18) remains high (54%). This suggests that sample 2.1 (60 mm thickness) may have also included grains from disturbed strata lying immediately below the buried ground surface, as observed with sample 3.1.2 (σ_b=44%) from a similar position relative to the buried ground surface. The values of overdispersion obtained with two of the upcast samples (20%, 1.1; 14%, 4.1.1) were sufficiently low to indicate they had also been sufficiently exposed to daylight before burial to be considered as well bleached. Hence for the above samples (2.1, 3.1.1, 1.1 and 4.1.1) the use of the CDM to calculate the weighted mean value of D_e was judged appropriate.

With the exception of the two samples mentioned above, the D_e distributions for the upcast samples exhibited high levels of overdispersion, ranging from 35% to 93% (Table 1). Consequently, in combination with an assessment of their skewness, these samples were assessed for the suitability of application of the minimum dose or finite mixture models. Although positive skewness is generally associated with sediment deposited under conditions of rapid deposition, leading to partial bleaching of a population of grains, skewness of differing polarity could arise with upcast deposits. The process of dumping of upcast on the mound has the potential to give rise to heterogeneity in the internal structure of the mound, and the spatial scale on which this occurs will be related to the volume of the upcast container (e.g., a bucket). In turn, the uniformity of exposure of grains within such volumes that are subsequently analysed is likely to be highly variable, depending on processes of mechanical dispersal, settling, disturbance, their location relative to an exposed surface, and also the length of time until the next deposition of upcast. Hence the 'spectrum' of the degree of bleaching of grains may vary considerably within a mound, where moving from a minority to a majority of well-bleached grains could be expected to cause the skewness to change from negative to positive polarity depending on the proportions of well and poorly bleached grains. Other known potential issues such as underestimating the depth of penetration of sunlight beneath the exposed surface during the existence of the mound or during excavation would also compound this issue.

Although only one sample (1.2 ; c/c_{crit} =144%, positive; all values given in Supplementary Material Table SM3b) exhibited a statistically significant value of skewness for aliquots containing a dominant individual bright grain (1gr), seven other samples, had high positive values (2.2, 60%; 4.1.2, 86%; 4.1.3, 49%; 3.1.2, 72%; 3.1.3, 60%; 3.1.4, 66%) and a negative value in the case of sample 4.1.3 (49%). The aliquots with more than one bright grain (2-4 gr), exhibit mixed behaviour (Supplementary Material, Table SM3b) although there is a general shift in the D_e distributions to both higher D_e values, consistent with grain averaging effects, and one sample showed no significant change (4.1.2). To enable a comparison of characteristics, the overall distribution of values of overdispersion and skewness for the Bureta samples are plotted in Fig. SM4c (Supplementary Material). For these seven samples showing both high overdispersion, and combined with a degree of skewness, the MDM was judged to be appropriate.
There are two further upcast samples – 1.3 and 2.2 – where the values of the descriptive statistical parameters were initially less clear cut. In the case of sample 2.2, the D_e distribution exhibits both high overdispersion (73%) and tendency to positive skewness (60%). There is a preponderance of D_e values in the proximity of the central value (CDM) in the two distributions of D_e values obtained with aliquots containing an individual bright grain

and with the addition of aliquots containing several grains (2-4 gr), a minimum dose component could also be defined in the radial plot (Supplementary Material, Fig. SM4c). In this case application of the FMM yielded a total of three fitted D_e components, two of which are relevant to age calculation (Table 1). The D_e distribution (1gr) for sample 1.3 also exhibited high overdispersion (σ_b=42%), but only a slight tendency to positive skewness (26%); the D_e distribution for aliquots containing up to several grains (2-4 gr) has a lower value of OD (30%) and negligible skewness (2%). In this case the application of the CDM was judged to be a reasonable compromise for a sample that was not in a critical stratigraphic position.
Given the above considerations concerning the upcast samples, the MDM was judged to be the most appropriate model to apply to calculate the weighted mean value of D_e for all upcast samples (Table 1), with the exception of samples 1.3, 1.1 and 4.1.1.

5.6.3 Dose rate

The values of the average total burial dose rate, $\dot{D}_{tot}$, and its components, $\dot{D}_{\beta+ig}$ and $\dot{D}_{\gamma+cos}$, for each sample are listed in Table 1. $\dot{D}_{\beta+ig}$ represents the average beta dose rate, corrected for attenuation effects and average moisture content (Aitken, 1985), and includes a calculated contribution (0.035 mGy a^{-1}) to account for trace quantities of radionuclides within the grains. $\dot{D}_{\gamma+cos}$ represents the combined γ and cosmic burial dose rate, corrected for moisture content and each component of this combined dose rate, $\dot{D}_{\gamma}$ and $\dot{D}_{cos,}$ corresponds to the time-averaged value of the burial dose rate for each sample following the procedure outlined in Section 4.4. The values of the average specific activities (Bq kg^{-1}) of the sediment samples used in these calculations are listed in the Supplementary Material (Table SM3c).

5.6.4 OSL ages

The OSL ages in Table 1 (col. 11) are given in years (a, annum) before 2014, together with the type A ($\pm\sigma_A$) and B ($\pm\sigma_B$) standard uncertainties (ISO 1993) calculated at the 68% level of confidence (1σ), rounded to the nearest 5 years. Two depositional ages were calculated for sample 2.2 where the FMM model was applied, as discussed in the previous section.

6. Interpretation

The OSL ages obtained for samples taken from a) the two shaft mounds S2 and S4 that formed part of the initial fieldwork and b) mound S3 and a second section of mound S2 are shown as calendrical dates with their stratigraphic positions in Fig. 3, where the depths indicated are relative to the present ground surface.
In addressing the question of whether a chronostratigraphy had been preserved in the shaft mounds, the date estimates for the burial of the ground surface by the upcast deposits during construction of the qanat are expected to be similar for comparable deposits within each mound. The OSL ages for all four sections are generally in stratigraphic order, showing an overall increase in age with depth and we first discuss the results for the mound S2 where two sections were cut to test for concordance.

The OSL dates for the basal upcast deposits within the two sections of the same mound (S2), of AD 1230±70 (Loc. 3.1.2) and AD 1350±55 (Loc. 2.1), are in agreement (T=2.4; σ_A; $\chi^2_{1,0.05}$ = 3.84) using Ward and Wilson's (1978) test statistic, T. Hence they produce a consistent estimate of the date of deposition of the initial upcast. In the overlying upcast deposits, the OSL date estimates of AD 1430±125 (3.1.4) and AD 1390±50 (2.2) are similar (T= 0.1; σ_A; $\chi^2_{1,0.05}$ = 3.84) and also produce consistent results for a comparable layer within the same mound, notwithstanding the relatively large uncertainty associated with the former. Since comparison of these OSL ages in each section of mound S2 does not reveal statistically significant differences (3.1.4 vs 3.1.3; T= 0.1; σ_A; $\chi^2_{1,0.05}$ = 3.84; 2.2 vs 2.2L; T= 2.0; σ_A; $\chi^2_{1,0.05}$ = 3.84), these results suggest that the deposits within the initial ca 10 cm of upcast in this mound are coeval. Lying ~10 cm above sample 2.2, and yet ~70 cm below the crest of the extant mound S2 in section 391-2, sample 2.3 yielded a modern date estimate

(ca 50 years old), reflecting the potential for discontinuity in the preserved sedimentary record within the mounds. Tests with quartz grains from the deposits located immediately above sample 2.3 (sample 2.4) and lying ca 10 cm below the present ground surface in this mound indicated that they were not sufficiently exposed to daylight before burial to enable an estimate of burial age to be obtained. Although the results for sample 2.2 reflect a high luminescence sensitivity of quartz grains in upcast from this site and suggest a potential for dating relatively recent burial events, the grains were poorly bleached (σ_b=93%) and the extent to which recently deposited sediments would have remained undisturbed in contexts of this type is untested.

In contrast, the basal deposits of upcast in the other two mounds (S3 and S4) produced OSL dates that are significantly younger (S3; Loc. 4.1.3, AD 1715±70 and S4; 1.1, AD 1550±40) than those for comparable deposits in mound S2. In the sampled block of mound S3, sample 4.1.3 was taken ca 6 cm above the contact to avoid root activity in the deposits overlying the indicated horizon, and consequently the date obtained could reflect a later deposition. The OSL date obtained for sample 4.1.5 (AD 1630±135), has high uncertainty and clearly overlaps the date for 4.1.3. Putting the date for 4.1.5 to one side because of its relative large uncertainty estimate, the OSL dates for the underlying samples (4.1.3, 4.1.2 and 4.1.1, which do form a coherent group; T= 10.6; σ_A; $\chi^2_{2,0.05}$ = 5.99) form a co-linear trend with increasing depth with an average aggradation rate of ca 1.6 cm per decade. Since examination of the thin section (Section 3) identified the putative horizon between samples 4.1.2 and 4.1.3 as a contact between two phases of upcast accumulation, with evidence for a period of stabilisation, the degree to which OSL in combination with micromorphological analysis can differentiate phases of deposition will be the subject of further investigation. In mound S4, only samples lying above the buried ground surface were collected. The OSL dates for the basal deposit sample 1.1 (AD 1550±40) and sample 1.2 (AD 1700±25) lying ca 11 cm above the horizon indicate that they are not coeval (T= 19.8; σ_A; $\chi^2_{1,0.05}$ = 3.84), but this ca 150 year span during the late medieval period for the basal upcast is broadly consistent with that obtained in mound S3, and both contrast with the earlier chronology obtained in mound S2. One explanation for this chronometric discordance may lie in the effect of weathering processes that have eroded the mounds and shafts. Although it was not feasible to undertake a detailed examination of the internal structure of each mound, a degree of elongation of the mound perimeter and asymmetry in the positioning of the shaft bore was evident, and the position of the sections were selected with the aim of avoiding strata affected by erosion, as discussed above. However, progressive erosion of part (or all) of the upper shaft and mound leading to collapse of sediment into the tunnel would enlarge the shaft throat, and reinstating a mound is likely to have caused the summit of the mound to move further away from the central axis of the original shaft, depending on the extent of the erosion. In this process, the original horizon between the ground surface and the upcast is likely to have been disturbed and eventually lost (Fig. 3b). If the internal structure of mounds S3 and S4 had been affected in this way, it is plausible that the depositional process dated by OSL represents a later rebuilding of the mound, in this case during the early 16th century. It is noticeable that the buried ground surface horizons identified in the sections of mounds S3 (-40 cm) and S4 (-60 cm) are 20-30 cm deeper than those recorded in the sections of mound S2 (Loc. 3, -20 cm and Loc. 2, 30 cm), and investigation of whether these deeper deposits represent backfill following erosion would require more extensive excavation of the mounds. If this suggested mechanism is valid, the OSL results for mounds S3 and S4 suggest significant activity in rebuilding of these mounds during the late 16th /early 17th centuries, with sediment deposition on the mounds continuing for a further couple of hundred years.

7. Conclusion

As a pilot investigation, this study has successfully demonstrated the potential for applying OSL techniques to the dating of sedimentary deposits within the surface mounds of qanat shafts. It has also underlined the importance of understanding the internal structure of the

mounds by micromorphological analysis of thin sections prepared from excised blocks of sediment. While comparison of OSL dates for three different mounds in the Bureta qanat suggest that each may contain a different depositional history, the concordance of the OSL dates including the 13th century AD date for the basal upcast obtained from two different sections of the same mound, suggests that they are at least consistent. Testing of their accuracy will require the dating of qanats with independent dating evidence for construction and such (rare) sites are being sought. The finding of partial bleaching of grains before burial in most of the sampled upcast deposits (and also in the uppermost palaeosol deposits) confirms the need for measurements with individual grains in future work on qanat mounds, although a more detailed analysis of the effect of grain-averaging in small aliquots on the weighted average value of the equivalent dose may enable a reduction in the lengthy instrument time required for measurements of this type. The later depositional dates for upcast in the case of mounds S3 and S4 suggest that they were rebuilt during the 16th century and this has also given rise to the presence of upcast deposits at greater thickness. For mound S2, the boundary between palaeosol and upcast (confirmed by sediment thin-section analysis) was found to lie 20-30 cm below the current ground surface and this gives some hope that a preserved contact may have survived in cases where the contemporary shaft mounds were levelled by ploughing. In commencing to build a methodological basis for dating qanat construction and use, we realise that shaft mounds may vary greatly in form and composition (M. Antequera, pers. comm.) elsewhere in Spain, notably in the South, and accommodating these presents an interesting challenge.

Acknowledgements
This research was supported by the University of Durham. The authors thank Soledad and Malaquías Lores for allowing access and permission to study the qanat, and the Ayuntamiento de Bureta (Zaragoza) for its help and support. Isidro Aguilera first introduced the authors to the Bureta qanat. Discussions with Prof. T.W. Wilkinson regarding the dating of irrigation features were instrumental in initiating OSL work.

References

Adamiec, G., Aitken, M.J., 1998. Dose rate conversion factors: update. Ancient TL 16, 37-50.
Aitken, M.J., 1985. Thermoluminescence Dating. Academic Press, London.
Aitken, M.J., 1998. An introduction to optical dating. Oxford University Press, Oxford.
Arnold, L.J., Roberts, R.G., 2009. Stochastic modelling of multi-grain equivalent dose (D_e) distributions: Implications for OSL dating of sediment mixtures. Quaternary Geochronology 4, 204-230.
Arnold, L.J., Demuro, M., Nvazo Ruiz, M., 2012. Empirical insights into multi-grain averaging effects from 'pseudo' single-grain OSL measurements. Radiat. Measurements 47, 652-658.
Bailey, R.M., Arnold, L.J., 2006. Statistical modelling of single grain quartz D_e distributions and an assessment of procedures for estimating burial dose. Quaternary Science Reviews 25, 2475-2502.
Bailiff, I.K., 2007. Methodological developments in the dating of brick from late medieval and post medieval English buildings. Archaeometry 49, 827-851.
Bailiff, I.K., French, C.A., Scarre, C.J., 2014. Application of luminescence dating and geomorphological analysis to the study of landscape evolution, settlement and climate change on the Channel Island of Herm. J. Arch. Science 41, 890-903.
Ballarini, M., Wallinga, J., Wintle, A.G., Bos, A.J.J., 2007. A modified SAR protocol for optical dating of individual grains from young quartz samples. Radiation Measurements 42, 360-369.
Bateman, M.D., Boulter, C.H., Carr, A.S., Frederick, C.D., Peter, D., Wilder, M., 2007. Detecting post-depositional sediment disturbance in sandy deposits using optical luminescence. Quaternary Geochronology 2, 57-64.
Berger, G. W., Post, S., Wenker, C. 2009. Single and multigrain quartz-luminescence dating of irrigation-channel features in Santa Fe, New Mexico. Geoarchaeology 24, 383-401.
Bullock, P., Fedoroff, N., Jongerius, A., Stoops, G., Tursina, T., Babel, U., 1985. Handbook for Soil Thin Section Description.Waine Research Publications, Albrington.Burillo, F., M. Gutiérrez, J.L. Peña and C. Sancho 1986 Geomorphological processes as indicators of climatic changes

during the Holocene in north-east Spain. In F. López-Vera (ed.), Quaternary Climate in Western Mediterranean, 31-44. Madrid: Universidad Autónoma de Madrid.
Burillo, F., Gutiérrez, M., Peña, J.L., Sancho, C., 1986. Geomorphological processes as indicators of climatic changes during the Holocene in north-east Spain. In F. López-Vera (ed.), Quaternary Climate in Western Mediterranean, 31-44. Madrid: Universidad Autónoma de Madrid.
Courty, M-A., Goldberg, P., Macphail, R.I.,1989. Soils and micromorphology in archaeology. Cambridge, Cambridge University Press.
English, P W., 1968. The origin and spread of qanats in the Old World, Proceedings of the American Philosophical Society 112, 170-81.
Fattahi, M., Aqazadeh, A., Walker, R.T., Talebian, M., Sloan, R.A., Khatib, M.M. , 2011. Investigation on the Potential of OSL for dating qanat in the Dasht-e Bayaz region of north-eastern Iran using the SAR protocol for quartz. J. Seismology and Earthquake Eng. 13, 65-75.
Galbraith, R.F., Roberts, R.G., Laslett, G.M., Yoshida, H., Olley, J.M., 1999. Optical dating of single and multiple grains of quartz from Jinmium rock shelter, Northern Australia: part 1, experimental details and statistical models. Archaeometry 41, 339-364.
Gerrard, C.M., 2011. Contest and co-operation: strategies for medieval and later irrigation along the Huecha Valley, Aragón, north-east Spain. Water History 3(1), 3-28.
Gerrard, C.M., Gutiérrez, A., 2012. Estudio arqueológico del Somontano del Moncayo: avance metodológico. Salduie: Estudios de prehistoria y arqueología 10, 259-270.
Glick, T.F., 1970. Irrigation and Society in Medieval Valencia. Cambridge, Mass., Harvard University Press.
Gutiérrez, M., Peña, J.L., 1998 Geomorphology and Upper Holocene climatic change in Northeastern Spain. Geomorphology 23, 205-17.
Jacobs, Z., Duller, G.A.T., Wintle, A.G., 2006. Interpretation of single grain D_e distributions and calculation of De. Radiation Measurements 41, 264-277.
Huckleberry, G., Hayshida, F., Johnson, J. 2012. New insights into the evolution of an intervalley prehistoric irrigation canal system, north coastal Peru. Geoarchaeology 27 (6), 492-520.
Huckleberry, G., Rittenour, T. 2014. Combining radiocarbon and single-grain optically stimulated luminescence methods to accurately date pre-ceramic irrigation canals, Tuscon, Arizona. Journal of Archaeological Science 41, 156-170.
ISO, 1993, International vocabulary of basic and general terms in metrology. 2nd Edition. International Organisation for Standardization, Geneva, Switzerland.
Jones, A. P., Tucker, M. E., Hart, J. K., 1999. The description and analysis of Quaternary stratigraphic sections, Technical Guide 7; Quaternary Research Association, London, 293pp.
Munsell Color Co., Inc., 1952, Munsell soil color chart: Baltimore, Md., USA.
Murray, A.S., Wintle, A.G., 2000. Luminescence dating of quartz using an improved single-aliquot regenerative-dose protocol. Radiation Measurements 32, 57-73.
Murray, A.S., Wintle, A.G., 2003. The single aliquot regenerative dose protocol: potential for improvements in reliability. Radiation Measurements 37, 377-381.
Peña, J.L., Echeverría, M.T., Julián, A. , Chueca, J., 2000. Processus d'accumulation et d'incision pendant l'Antiquité Classique dans la vallée de la Huerva (Bassin de l'Ebre, Espagne). In F. Vermeulen and M. de Dapper (eds.), Geoarchaeology of the Landscapes of Classical Antiquity. Babesch Supplement 5, 151-60. Leiden: Stichting Babesch.
Reineck, H, E. , Singh, I, B., 1980. Depositional Sedimentary Environments. Springer- Verlag Berlin Heidleberg. 2nd edition.
Rittenour, T.M., 2008. Luminescence dating of fluvial deposits: applications to geomorphic, palaeoseismic and archaeological Research. Boreas 37, 613-635.
Stoops, G., Marcelino, V., Mees, F. 2010. Interpretation of Micromorphological Features of Soils and Regoliths. Elsevier, Amsterdam, pp. 329-350.
van Der Meer, J,J, M., Menzies, J. , 2011. The micromorphology of unconsolidated sediments. Sedimentary Geology, 238, 213-232.
Ward, G.K., Wilson, S.R., 1978. Procedures for comparing and combining radiocarbon age determinations: a critique. Archaeometry 20, 19-31.
Wilkinson, K.N., Gerrard, C.M., Aguilera, I., Bailiff, I., Pope, R.J.J., 2005. Prehistoric and historic landscape change in Aragón, Spain: some results from the Moncayo Archaeological Survey. J. Mediterranean Archaeology 18.1, 31-54.
Wintle, A.G., Murray, A.S., 2006. A review of quartz optically stimulated luminescence characteristics and their relevance in single-aliquot regeneration dating protocols. Radiation Measurements 41, 369-391.

Table 1. OSL ages and related data

		Dose rate			Equivalent. dose					
Lab #	Type	$\dot{D}_{\beta+ig}$ ±s.e.	$\dot{D}_{\gamma+cos}$ ±s.e.	$\dot{D}_{tot}$ ±s.e.	OD σ_i	OD σ_b	n 1g	D_e ±s.e.	Model	OSL Age $\pm\sigma_A$; $\pm\sigma_B$
390-		(mGy a^{-1})	(mGy a^{-1})	(mGy a^{-1})	%	%		(Gy)		(a)
1.3	UC	1.53±0.08	1.15±0.06	2.68±0.10	11	42	14	0.58±0.07	CDM	215 ±27; ±30
1.2	UC	1.56±0.08	1.25±0.06	2.81±0.10	5	54	16	0.89±0.04	MDM	315 ±18; ±25
1.1	UC	1.41±0.70	1.02±0.05	2.43±0.09	10	20	16	1.12±0.07	CDM	460 ±33; ±42
2.3	UC	1.43±0.07	1.22±0.06	2.66±0.09	10	93	9	0.14±0.01	MDM	55 ±10; ±10
2.2	UC	1.71±0.09	1.15±0.06	2.86±0.10	10	73	19	1.80±0.06	FMM	625 ±30; ±50
								0.72±0.05	"	250 ±20; ±25
2.2L	UC	1.43±0.07	1.06±0.05	2.49±0.09	10	35	10	1.76±0.11	MDM	705 ±48; ±65
2.1	PS	1.53±0.08	0.99±0.05	2.52±0.09	13	46(0)*	4*	4.64±0.33	CDM	1840 ±145; ±180
3.1.4	UC	1.51±0.08	1.20±0.06	2.71±0.10	13	56	9	1.59±0.32	MDM	585 ±120; ±125
3.1.3	UC	1.48±0.07	1.21±0.06	2.69±0.10	7	54	29	2.12±0.12	MDM	790 ±50; ±70
3.1.2	PS	1.41±0.07	1.22±0.06	2.63±0.09	12	44	15	2.46±0.66	MDM	940 ±255; ±260
3.1.1	PS	1.38±0.07	0.91±0.05	2.29±0.08	7	29 (21)*	12*	6.00±0.42	CDM	2620 ±200; ±250
4.1.5	UC	1.93±0.10	1.32±0.07	3.25±0.12	20	91	10	1.25±0.43	MDM	385 ±130; ±135
4.1.3	UC	1.70±0.09	1.18±0.06	2.87±0.10	7	72	18	0.85±0.19	MDM	300 ±65; ±70
4.1.2	UC	1.41±0.07	1.17±0.06	2.58±0.09	5	76	18	1.06±0.09	MDM	410 ±37; ±45
4.1.1	UC	1.46±0.07	1.16±0.06	2.62±0.09	12	14	4	1.35±0.07	CDM	515 ±32; ±43
(1)	(2)	(3)	(4)	(5)	(6)	(7)	(8)	(9)	(10)	(11)

Notes.

1. The two types of deposit indicated in col. 2 correspond to upcast (UC) and palaeosol (PS).
2. The values (col. 3) of the combined external beta and internal grain dose rate, $\dot{D}_{\beta+ig,}$ include an allowance of 0.035 mGy a^{-1} for the internal grain dose rate (alpha and beta) arising from radionuclides within the quartz. The combined gamma and cosmic dose rate (col. 5), $\dot{D}_{\gamma+cos}$, takes into account the time-dependent development of overburden. Corrections for average moisture content have been applied to both beta and gamma dose rates The calculated dose rates are shown rounded to 2 decimal places.
3. The statistical parameters listed in cols 6-8 correspond to the intrinsic uncertainty (σ_i), the extrinsic uncertainty represented by the overdispersion (σ_b) and the number of aliquots (n) containing one dominant bright grain (1gr). The weighted value of the equivalent dose, D_e, is given in col. 9, together with the standard error calculated using the model indicated in col. 10, where CDM denotes the Central Dose Model, CDM, the Finite Mixture Model, FMM and MDM, the Minimum Dose Model, as discussed in the main text.
4. The asterisk marked against values of σ_b and n for samples 2.1 and 3.1.1 indicate recalculated values after removal of one outlying D_e value in each case.
5. The reference year for age calculation is AD 2014; the standard errors σ_A and σ_B are given at the 68% level of confidence (1σ).

Figure 1

The site of Bureta, located in Aragón, is one of the most northerly qanat sites in Spain.

Figure 2

Sections of shaft mounds indicating the main Stratigraphic Units (SU) and sample locations in mounds S2 and S3.

A) Shaft mound S2, (1) Upcast, Silty loam; (2) Upcast, silty clay; (3) Upcast, silty clay; (4) Palaesol, Silty sand.

B) Shaft mound S3, (1) Upcast, Silty clay; (2) Humic layer, silty clay; (3) Upcast, Sandy silt; (4) Upcast, Clay; (5) Humic layer, silt; (6) Upcast, Silty clay; (7) Upcast, silty clay.

A more detailed description of the Stratigraphic Units is provided in the Supplementary Material (Section 2).

A)

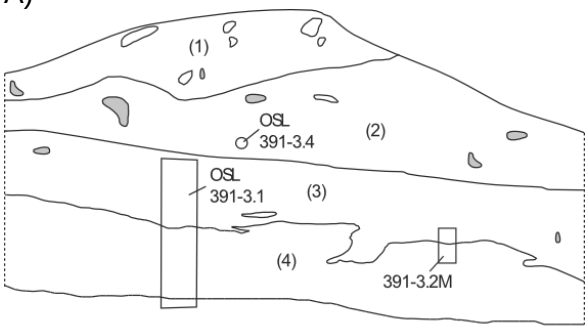

A) S2, North facing section

B)

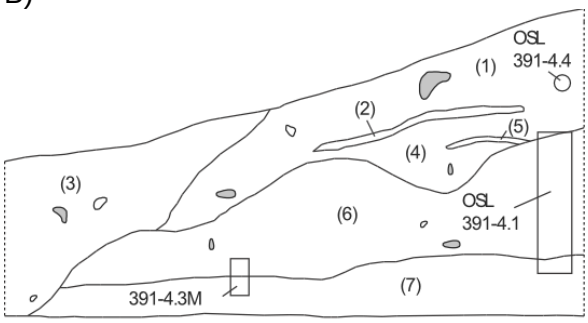

B) S3, South facing section

Figure 3.

a) Stratigraphy and OSL sample locations shown for the three shaft mounds tested (S2- S4), where four sections were sampled (391 -1, -2, -3 and -4). The depths shown are below the current ground surface; the elevation of the top of the sections 391-3 and 391-4 of mounds S2 and S3 were recorded as 499.11 m and 498.14 m respectively, measured using a Leica Zeno digital GPS. The solid red line in the columns represents a horizon boundary as identified visually during the excavation. The positions and vertical extension of the OSL samples are indicated as bars; the sample number within each section is indicated to the right of the column, together with the OSL age and overall error (σ_B, 1σ).

Inset b) Schematic illustration of erosion model for a qanat shaft mound, showing a cross section of the shaft and mound as formed after construction (I) and, rebuilding of the mound (II) after a prolonged period of erosion of the upper part of the shaft affecting part of the mound.